Bulg. J. Phys. **45** (2018) 275–284

Impedance, Modulus and Spectroscopic Analysis of Gel-Grown Pure Lead Levo-Tartrate Crystals

H.O. Jethva, M.J. Joshi
Department of Physics, Saurashtra University, Rajkot 360005, India

Received: *December 5, 2017*

Abstract. Various metal tartrate crystals find different applications. In the present study pure lead levo-tartrate crystals were grown by using silica hydro gel as the growth medium. Long, dendrite, dense and white crystals were grown at the gel-liquid interface. Using complex impedance spectroscopy (CIS) technique, the complex impedance (Z^*) and modulus (M^*) properties of the crystals were analyzed as a function of frequency within the range from 100 Hz to 400 kHz at room temperature. The complex impedance and modulus plots exhibited the presence of grain (bulk) as well as grain boundary contributions in the crystals. The M'' versus frequency plot revealed two peaks, while the Z'' versus frequency plot revealed only one peak. It has been found that these peaks are of Debye type nature.

PACS codes: 84.37.+q

1 Introduction

Many metal tartrates find various applications in different fields, for example, application of strontium tartrate as an important ferroelectric material [1], ferroelectric, dielectric, optical and thermal properties of calcium tartrate [2], application of iron tartrate as one of the prominent species in apple juice [3], piezoelectric application of cadmium tartrate [4] and addition of lead tartrate in gasoline to prevent knocking in motors [5]. The gel growth technique is found to be suitable to grow tartrate compound crystals [6] and many authors have reported the growth of metal tartrate crystals [6-10], mixed metal tartrate crystals [11-15] and ternary metal tartrate crystals [16,17]. For pure and mixed metal tartrate crystals, EDAX, FTIR, Powder XRD, TGA and dielectric characterizations have been reported but as far as the knowledge of the present authors is concern, very scanty reports are available in the literature regarding the impedance analysis of gel grown tartrate crystals [18,19] and no major reports are available in the literature regarding the modulus and spectroscopic analysis of gel grown tartrate

crystals. Hence, an attempt is made by the present authors to analyze the lead levo-tartrate crystals by impedance and modulus spectroscopy.

Complex impedance spectroscopy [20] is an effective experimental technique used to study the electrical behavior of the sample over a wide range of frequencies and temperatures. This method helps to separate real and imaginary components of the complex electrical parameters and provides a true picture of the material properties [21]. Using CIS method, one can resolve the relaxation contributions, like, bulk properties, grain-boundary properties and electrode interface effects of polycrystalline materials. If these materials have two or more contributions with different relaxation times, then two or more circular arcs are observed in their complex impedance plane plots of Z' versus Z'', where Z' and Z'' are the real and imaginary parts of the complex impedance plane, respectively, and the complex modulus plane plots of M' versus M'', where M' and M'' are the real and imaginary parts of the complex modulus plane, respectively [20,22-24]. The complex impedance plots are useful for determining the dominant resistance of a sample, but they are insensitive to the smaller values of the resistances, while the complex modulus plots are useful in determining the smallest capacitances. Sinclair and West [23] suggested the combined usage of impedance and modulus spectroscopic plots. The peak heights of the spectroscopic plots of Z'' versus frequency are proportional to R, i.e., it highlights the phenomenon of largest resistance, while M'' versus frequency plots are proportional to $1/C$, i.e., it highlights the phenomenon of the smallest capacitance.

2 Experimental

Sodium metasilicate solution of density 1.05 gm/cm^3 was used for the preparation of gel. Solution of 1 M levo-tartaric acid was mixed with the solution of sodium metasilicate and the pH of the mixture was set at 4.5. The mixture was poured in the test tubes of 2.5 cm diameter and 14 cm length to set into the gel. The gel was set within 5 to 6 days and then supernatant solution of 1 M, 10 ml lead nitrate (anhydrous) solution was gently poured on the set gel without disturbing the gel surfaces.

All the chemicals were AR grade and obtained from Ranbaxy chemicals. The following reaction is expected to occur.

$$\mathrm{Pb(NO_3)_2 + H_2C_4H_4O_6 + nH_2O \rightarrow PbC_4H_4O_6 \cdot nH_2O + 2HNO_3}$$

The amount of HNO_3 produced is very less in comparison to the nutrients being supplied to the growing crystals and hence no major limitation is imposed on the growth of crystals [8,11-14,16,17].

The growth of crystals near the gel-liquid interface was completed within twenty days. The crystals were dendrite type, dense, long and white. The growth of crystals inside the test tube is shown in Figure 1.

Figure 1. Growth of lead levo-tartrate dendrite crystals in test-tube.

3 Characterization Technique

The synthesized sample was ground to very fine powder and made the pellet without any binder. As the sample is organo-metallic compound, it may react with the conductive layers of the coating material, the pellet without any coating was used for the impedance measurement. The density and porosity of the pellet was not measured but the pellet was prepared by applying a pressure of 5 ton/cm^2. The pellet was sandwiched between two identical, circular, smooth and cleaned electrodes under spring pressure to ensure good electrical contacts between the electrodes and the sample, so that the parasite capacitance induced by the presence of air interstices at the interfaces between the sample and the electrode can be avoided. The real and imaginary parts of complex impedance were measured for the pelletized sample as a function of frequency ranging from 100 Hz to 400 kHz at room temperature using SI-1260 Solartron impedance/gain phase analyzer. The inbuilt software controls the measurements and calculates the real and imaginary parts of impedance. The real (Z') and imaginary (Z'') parts of complex impedance (Z^*) were used for the evaluation of the real (M') and imaginary (M'') parts of complex electric modulus (M^*) using the equations [25]:

$$Z^* = Z' - jZ'' , \tag{1}$$

$$M^* = j\omega C_0 Z^* = M' + jM'' . \tag{2}$$

From equations (1) and (2) the equations of real part and imaginary part of complex electric modulus (M^*) can be obtained as:

$$M' = \omega C_0 Z'' , \tag{3}$$

$$M'' = \omega C_0 Z' . \tag{4}$$

In the equations (2), (3) and (4), $\omega = 2\pi f$ is the angular frequency, f is the frequency of the applied field and C_0 is the vacuum capacitance of the measuring cell and electrodes with an air gap of the dimension of the sample thickness. $C_0 = \varepsilon_0 A/t$, where ε_0 is the permittivity of free space (8.85×10^{-12} F/m), t and A are the thickness and the cross-section area of the sample, respectively.

4 Result and Discussion

4.1 Frequency dependence of Z' and M' at room temperature

Figure 2 shows the frequency dependence of real (Z') and real (M') components of the complex impedance and complex modulus at room temperature, respectively, for the pure lead levo tartrate crystals. It is observed from the plot that the dispersion in the value of Z' within the frequency range 100 Hz to 250 Hz is very small, which is mainly due to polarization and then within the frequency range 300 Hz to 5000 Hz, a dramatic decrease in the value of Z' is observed with increase in frequency. This indicates the increase in the ac-conductivity of the sample with the increase in frequency [26] and the presence of space charge conduction at low frequencies. This also indicates that the capacitive and the resistive components of the equivalent circuit are active in this range of frequencies [27]. At higher frequencies, the Z' achieves nearly a very low constant value and becomes almost independent of frequency, which indicates the inability of space charges to follow the high frequency fields [28,29].

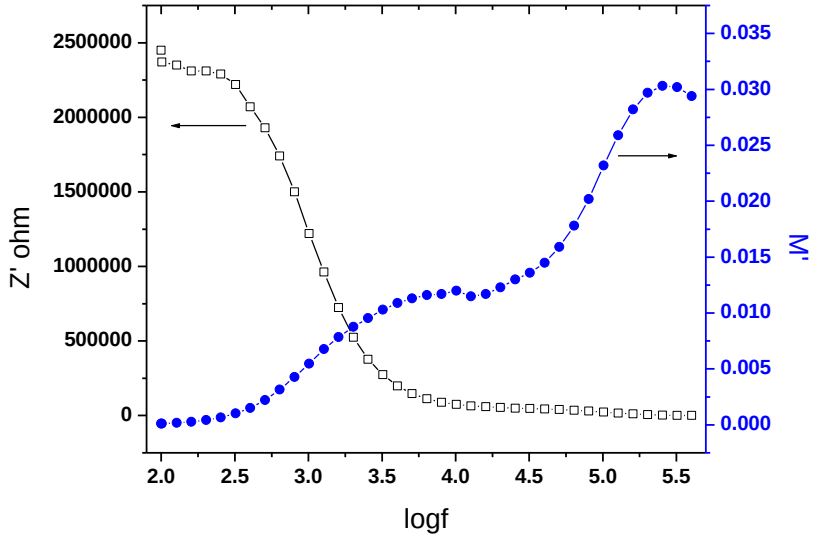

Figure 2. Plots of Z' versus $\log f$ and M' versus $\log f$.

At lower frequencies, the Z' decreases with the increase in frequency supporting a slow dynamic relaxation process in the sample, probably due to space charge that gets released at higher frequencies [28,30-33].

From the plot of M' versus $\log f$, it is observed that M' reaches almost a constant value at higher frequencies. At lower frequencies M' value is very small and tends to be zero indicating the removal of electrode polarization at the studied temperature [34,35]. The increasing value of M' with increasing frequency and reaching a maximum value M_∞ at high frequency, may be due to the distribution of relaxation processes over a range of frequencies [36]. The observed dispersion is mainly due to conductivity relaxation spreading over a range of frequencies and indicating the presence of a relaxation time, which is accompanied by a loss peak in the diagram of the imaginary part (M'') of electric modulus versus frequency. The absence of peak in M' diagram at room temperature within studied frequency range is due to the fact that M' in complex electric modulus (M^*) is equivalent to ε' in complex permittivity (ε^*), i.e., M' represents the ability of the material to store the energy [37]. The reduction in the value of M' at decreasing frequency results from the increase in the mobility of the charge carriers. It is well known that the orientation of the charge carriers and molecular dipoles becomes easier at low frequency.

4.2 Frequency dependence of Z'' and M'' at room temperature

Figure 3 shows the frequency dependence of imaginary (Z'') and imaginary (M'') components of the complex impedance and complex modulus at room temperature, respectively for the pure lead levo tartrate crystals.

The variation of Z'' with frequency reveals that Z'' value reaches a maximum $(Z''_{\max})$ and showing a relaxation or Debye-type peak. Such a behavior indicates the presence of relaxation in the sample. The appearance of the peak at low frequency side indicates the grain boundary relaxation mechanism in the sample. The peak height is proportional to the grain boundary resistance (R_{gb}), as expressed in the equation $Z'' = R_{\text{gb}}\omega_m\tau/1 + \omega_m^2\tau^2$, where ω_m is the relaxation angular frequency and τ is the relaxation time [38].

The plot of M'' versus $\log f$ shows two peaks at different frequencies. One at low frequency ~ 1011 Hz is attributed to the grain boundaries mechanism and another one at high frequency ~ 80380 Hz is attributed to the grain mechanism. These peaks explain a well defined two semicircles in the M^* plot. These peaks indicate the transition from short range to long range mobility, with decreasing frequency. The low frequency side of the peak represents the range of frequencies in which the ions are capable of moving long distances i.e., performing successful hopping from one site to the neighboring site, whereas for the high frequency side, the ions are spatially confined to their potential wells and can execute only localized motion [39]. According to ideal Debye theory of dielectric relaxation, the impedance (Z^*) and the modulus (M^*) maxima peaks occurs at

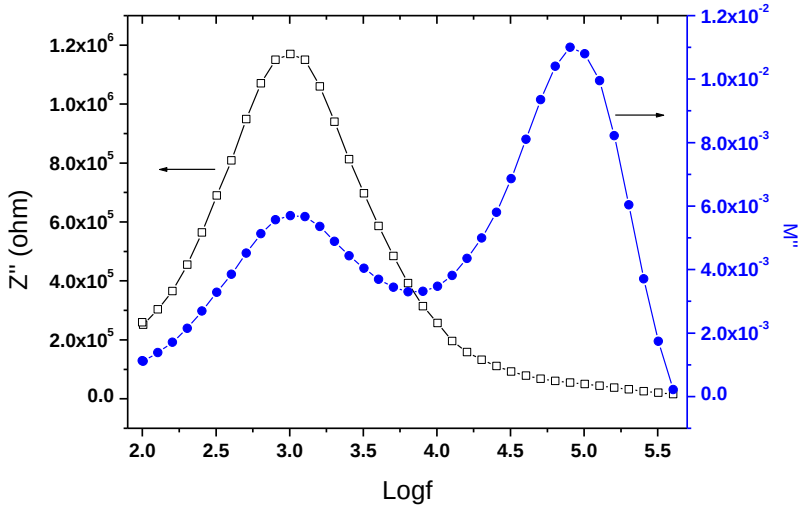

Figure 3. Plots of Z'' versus $\log f$ and M'' versus $\log f$.

the same frequency and the full widths at half maximum (FWHM) of these peaks should be less than 1.14 decades [40,41]. In the present case, the peaks of Z'' and M'' are observed at the same frequency ~ 1011 Hz and FWHM of Z'' and M'' are 1.0270 and 1.1303, respectively, i.e., less than 1.14 decades. This indicates that both the conditions are satisfied and hence, the observed relaxations are Debye-type.

4.3 Complex modulus spectrum

The complex modulus spectrum of pure lead levo-tartrate crystals at room temperature is shown in Figure 4. It is clear that the modulus plane shows two semicircles. The intercept of the first semicircle at low frequency side with the real axis indicates the total capacitance contributed by the grain boundary, while the intercept of the second semicircle at high frequency side indicates the total capacitance contributed by the grain [38]. From the intercepts of the plot on the real axis, the values of the grain boundary (C_{gb}) and grain (C_{g}) capacitances are found 59.5 pF and 40.5 pF, respectively.

4.4 Complex impedance spectrum

In order to obtain a better understanding of polarization mechanisms that exist in the pure lead levo-tartrate crystals at room temperature, complex impedance spectrum is drawn in Figure 5.

This plot allows the resistances related to grain, grain boundaries and

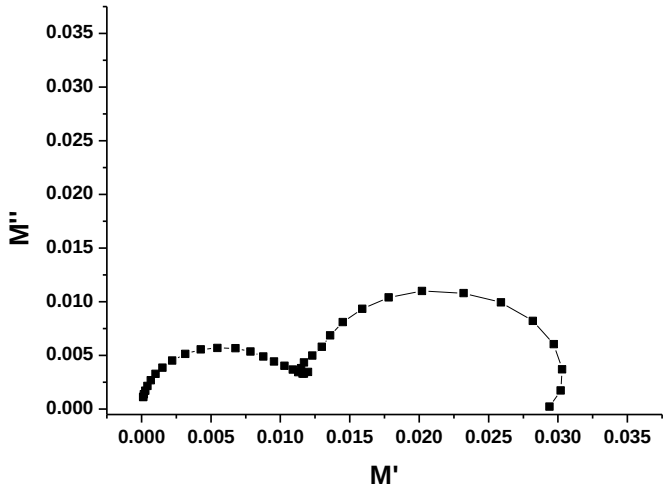

Figure 4. Complex modulus spectrum.

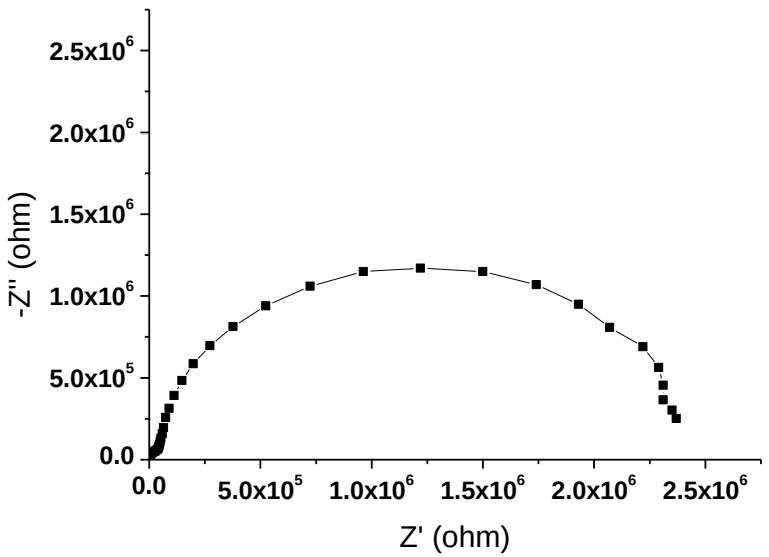

Figure 5. Complex impedance spectrum.

film/electrode interfaces to be separated because each of them has different relaxation times, resulting in separate semicircles in the complex impedance plane. In Figure 5, the complex plane illustrates two regions, which indicates different polarization mechanisms within the sample. At high frequencies nearer to the origin, the figure shows a semicircular arc, which is attributed to the electrical

properties of a parallel combination of bulk resistance and capacitance of the pure lead levo-tartrate crystals. At low frequencies away from the origin, the plot shows another semicircular arc, which is attributed to the distribution of grain boundary mechanism.

The complex modulus plot of Figure 4 shows two well observed semicircles and correspondingly two peaks in the plot of Figure 3 of M'' versus $\log f$, while the complex impedance plot of Figure 5 shows a very small semicircle near the origin at high frequency region and well observed semicircle at low frequency region but only one peak in the plot of Figure 3 of Z'' versus $\log f$. This is because depending upon the magnitudes of R and C components, different situations may arise. For instance, if one of the capacitances is much larger than the other, its associated peak and semicircle will effectively disappear from the modulus plot [42]. Similarly, if one of the resistances is much lower than the other, its associated peak and semicircle may effectively disappear or become too small to observe from the impedance plot. The key point in determining whether RC elements are detected depends on which plot is used and the relative magnitudes of the capacitances. The modulus plots give emphasis to those elements with the smallest capacitances, whereas the impedance plots highlight those with largest resistances [42].

In order to determine the values of the grain (R_{g}) and grain boundary (R_{gb}) resistances, the spectroscopic plot of M'' versus $\log f$ of Figure 3 is used. The plot shows two characteristic peaks. The peak at low frequency side corresponds to the grain boundary relaxation mechanism and satisfying the condition $2\pi f_{\max} R_{\mathrm{gb}} C_{\mathrm{gb}} = 1$, while the peak at high frequency side corresponds to the grain relaxation mechanism and satisfying the condition $2\pi f_{\max} R_{\mathrm{g}} C_{\mathrm{g}} = 1$. Here, $f_{\max}$ corresponds to the relaxation frequency associated with each mechanism. By these relations, R_{g} and R_{gb} are evaluated and found to be 48.9 kΩ and 2.64 MΩ, respectively. The very low value of grain resistance (R_{g}) compared to grain boundary resistance (R_{gb}) may be responsible for the non-appearance of corresponding peak in the spectroscopic plot of Z'' versus $\log f$ of Figure 3. The best fit equivalent circuit is shown in Figure 6, which is a parallel combination of R_{g}, C_{g} and R_{gb}, C_{gb} connected in series.

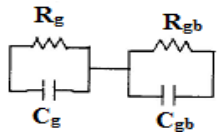

Figure 6. Equivalent circuit.

5 Conclusion

Lead levo-tartrate crystals were grown by using silica hydro gel as the growth medium. The long, dendrite, dense and white crystals were grown at the gel-liquid interface. The real and imaginary parts of complex impedance and modulus spectra of the lead levo-tartrate were investigated by using the complex impedance spectroscopy. The impedance and modulus plots showed the presence of grains as well as grain boundary contributions in the sample. The Z^* and M^* planes lead to lead levo-tartrate fit to the equivalent circuit composed of two parallel combinations of resistances and capacitances connected in series due to the grain and grain boundary mechanisms. The M'' versus frequency plot revealed two relaxation peaks, while the Z'' versus frequency plot revealed single relaxation peak and it was found that these peaks were a Debye-type.

Acknowledgement

The authors are thankful to Prof. H. H. Joshi (HOD, Department of Physics, Saurashtra University, Rajkot) for his motivation and keen interest and UGC for SAP DRS – III and DST for FIST.

References

[1] M.H. Rahimkutty, K. Rajendra Babu, K. Shreedharan Pillai, M.R. Sudarsana Kumar, C.M.K. Nair (2001) *Bull. Mater. Sci.* **24** 249.
[2] X. Sahaya Shajan, C. Mahadevan (2005) *Cryst. Res. Technol.* **40** 598.
[3] G. Weber (1991) *J. Anal. Chem.* **340** 161.
[4] J.S. Hopwood, A.W. Nicol (1972) *Crystallogr. J. Online.* **1600** 5767.
[5] N.J. Rahway (1952) "*The Merck Index of Chemicals and Drugs*", 6th ed. (Merck and Co.).
[6] H.K. Henish (1993) "*Crystal Growth in Gels*" (Dover Publication, New York).
[7] S.K. Arora, Vipul Patel, Brijesh Amin, Anjana Kothari (2014) *Bull. Mater. Sci.* **27** 141.
[8] H.O. Jethva, M.V. Parsania (2010) *Asian J. Chem.* **22** 6317.
[9] R.M. Dabhi, M.J. Joshi (2003) *Indian J. Phys.* **77** 481.
[10] S. Joseph, H.S. Joshi, M.J. Joshi (1997) *Cryst. Res. Technol.* **32** 339.
[11] H.O. Jethva, P.M. Vyas, K.P. Tank, M.J. Joshi (2014) *J. Therm. Anal. Calorim.* **117** 589.
[12] H.O. Jethva, M.J. Joshi (2014) *IJEIT* **4** 121.
[13] H.O. Jethva, M.J. Joshi (2014) *IJIRSET* **3** 16517.
[14] S.J. Joshi, B.B. Parekh, K.D. Parikh, K.D. Vora (2006) *Bull. Mater. Sci.* **29** 307.
[15] K.D. Parikh, B.B. Parekh, D.J. Dave, M.J. Joshi (2006) *Indian J. Phys.* **80** 719.
[16] S.J. Joshi, K.P. Tank, B.B. Parekh, M.J. Joshi (2010) *Cryst. Res. Technol.* **45** 303.

[17] S.J. Joshi, K.P. Tank, B.B. Parekh, M.J. Joshi (2013) *J. Therm. Anal. Calorim.* **112** 761.
[18] H.O. Jethva, M.J. Joshi, D.K. Kanchan (2015) *IJEIT* **5** 99.
[19] H.O. Jethva, D.K. Kanchan, M.J. Joshi (2016) *IJIRSET* **5** 221.
[20] J.R. Macdonald (1987) "*Impedance Spectroscopy*" (John Wiley and Sons, New York).
[21] M.J. Joshi (2017) *Mechanics, Materials Science & Engineering* **9** 261.
[22] D.C. Sinclair, A.R. West (1988) *J. Mat. Sci. Lett.* **7** 823.
[23] D.C. Sinclair, A.R. West (1989) *J. Appl. Phys.* **66** 3850.
[24] F.D. Morrison, D.C. Sinclair, A.R. West (1999) *J. Appl. Phys.* **86** 6355.
[25] K.P. Padmasree, D.K. Kanchan (2005) *Mater. Sci. Eng., B* **122** 24.
[26] A. Ala'eddin Saif, Zul Azhar Zahid Jamal, Zaliman Sauli, Prabakaran Poopalan (2011) *Mater. Sci. Medzg.* **17** 186.
[27] A. Ala'eddin Saif, P. Poopalan (2010) *J. Korean Soc.* **57** 1449.
[28] J. Plocharski, W. Wieczoreck (1988) *Solid State Ionics* **979** 28.
[29] Prasun Ganguly, A.K. Jha (2011) *Bull. Mater. Sci.* **34** 907.
[30] J. Suchanicz (1988) *Mater. Sci. Eng., B* **55** 114.
[31] C.K. Suman, K. Prasad, R.N.P. Chaudhary (2004) *Bull. Mater. Sci.* **27** 547.
[32] M.R. Rangaraju, R.N.P. Chaudhary (2004) *J. Mater. Sci.* **39** 1765.
[33] M. Rawat, K.L. Yadav, A. Kumar, P.K. Patel, N. Adhlakha, J. Rani (2012) *Adv. Mater. Lett.* **3** 286.
[34] F. Yakuphanoglu (2007) *Physica B* **393** 139.
[35] A. Dutta, T.P. Sinha, P. Jena, S. Adak (2008) *J. Non-Cryst. Solids* **354** 3952.
[36] L.N. Patro, K. Hariharan (2009) *Mater. Chem. Phys.* **116** 81.
[37] S.B. Aziz, Z.H.Z. Abidin, A.K. Arof (2010) *Express Polymer Letters* **4** 300.
[38] P.S. Sahoo, A. Panigrahi, S.K. Patri, R.N.P. Chaudhary (2010) *Materials Science-Poland* **28** 763.
[39] J.S. Kim (2001) *J. Phys. Soc. Jpn.* **70** 3129.
[40] K. Prabakar, S.A.K. Narayandass, D. Mangalaraj (2002) *Cryst. Res. Technol.* **37** 1094.
[41] A.R. James, C. Prakash, G. Prasad (2006) *J. Phys. D: Appl. Phys.* **39** 1635.
[42] D.C. Sinclair (1995) *Boi. Soc. Ceram. Vidrio* **34** 55.